Electronic Supplementary Material (ESI) for New Journal of Chemistry.
This journal is © The Royal Society of Chemistry and the Centre National de la Recherche Scientifique 2020

Electronic Supplementary Material (ESI)

A Squaraine-based Dipicolylamine Derivative Acting as a Turn-on Mercury(II) Fluorescent Probe in Water

Catarina V. Esteves,[a,†] Judite Costa,[b] Hélène Bernard,[c] Raphaël Tripier,[c] Rita Delgado[a]*

[a] *Instituto de Tecnologia Química e Biológica António Xavier, Universidade Nova de Lisboa, Av. da República, 2780–157 Oeiras, Portugal.*

[b] *Research Institute for Medicines (iMed.ULisboa, Faculdade de Farmácia, Universidade de Lisboa, Av. Prof. Gama Pinto, 1649-003 Lisboa, Portugal.*

[c] *Université de Brest, UMR-CNRS 6521, SFR SIBSAM, UFR des Sciences et Techniques, 6 avenue Victor le Gorgeu, C.S. 93837 29238 Brest Cedex 3, France.*

*E-mail: delgado@itqb.unl.pt

Table S1. Squaraine-based sensors for Hg^{2+} from the literature and the working medium used

Reference	Authors	Medium
9a	G. Wang *et al.*	EtOH/water solutions and pH 7.0 PBS buffer solution
9b	X. Liu *et al.*	DMSO, AcOH and SDS solutions
9c	S. Lee *et al.*	MeCN
9d	H. Zhu *et al.*	0.005% TW-80 (Tween-80 or polysorbate 80) at pH 5.0 PB buffer solutions
9e	H.-S. So *et al.*	MeCN
9f	S.-Y. Lin *et al.*	EtOH/water solutions
9g	B. A. Rao *et al.*	MeCN
9h	Q. Lin *et al.*	EtOH/water (30:70, v/v) solutions
9i	L. Hu *et al.*	DMSO/water (1:1, v/v) solutions and pH 8.0 PB buffer with 0.01 mol L^{-1} CTMAB (cetyltrimethylammonium bromide)
9j	K. M. Shafeekh *et al.*	MeOH
9k	C. Luo *et al.*	MeCN and MeCN/water (2:1, v/v) solutions
9l	C. Chen *et al.*	AcOH and AcOH/water (10:90, v/v) solutions
9m	C. Chen *et al.*	AcOH/water (40:60, v/v) solution
9n	Y. Xu *et al.*	Aqueous solution with cucurbit[8]uril (CB8)
9p	M. C. Basheer *et al.*	DCM
9q	J. V. Ros-Lis *et al.*	MeCN/water (1:4, v/v) pH 9.6 CHES buffer solutions
9r	J. V. Ros-Lis *et al.*	MeCN/water (20:80, v/v) pH 6.9 HEPES buffer solutions

9 (*a*) G. Wang, W. Xu, H. Yang and N. Fu, Highly Sensitive and Selective Strategy for Imaging Hg^{2+} Using Near-Infrared Squaraine Dye in Live Cells and Zebrafish, *Dyes and Pigments,* 2018, **157**, 369–376; *(b*) X. Liu, N. Li, M. M. Xu, C. Jiang, J. Wang, G. Song and Y. Wang, Dual Sensing Performance of 1,2-Squaraine for the Colorimetric Detection of Fe^{3+} and Hg^{2+} Ions, *Materials*, 2018, **11**, 1998; *(c*) S. Lee, B. A. Rao and Y.-A. Son, A Highly Selective Fluorescent Chemosensor for Hg^{2+} Based on a Squaraine–bis(rhodamine-B) Derivative: Part II, *Sensors and Actuators B: Chemical*, 2015, **210**, 519–532; *(d*) H. Zhu, Y. Lin, G. Wang, Y. Chen, X. Lin and N. Fu, A Coordination Driven Deaggregation Approach toward Hg^{2+}-specific Chemosensors Based on Thioether Linked Squaraine-Aniline Dyads, *Sensors and Actuators B: Chemical*, 2014, **198**, 201–209; *(e*) H.-S. So, H.-S. So, B. A. Rao, J. Hwang, K. Yesudas and Y.-A. Son, Synthesis of Novel Squaraine–bis(rhodamine-6G): A Fluorescent Chemosensor for the Selective Detection of Hg^{2+}, *Sensors and Actuators B: Chemical*, 2014, **202**: 779–787; *(f*) S.-Y. Lin, H.-J. Zhu, W.-J. Xu, G.-M. Wang and N.-Y. Fu, A Squaraine Based Fluorescent Probe for Mercury Ion via Coordination Induced Deaggregation Signaling, *Chinese Chem. Lett.*, 2014, **25**, 1291–1295; *(g*) B. A. Rao, H. Kim and Y.-A. Son, Synthesis of Near-Infrared Absorbing Pyrylium-Squaraine Dye for Selective Detection of Hg^{2+}, *Sensors and Actuators B: Chemical*, 2013, **188**, 847–856; *(h*) Q. Lin, Y. Huang, J. Fan, R. Wang and N. Fu, A Squaraine and Hg^{2+}-based Colorimetric and "Turn on" Fluorescent Probe for Cysteine, *Talanta*, 2013, **114**, 66–72; *(i*) L. Hu, Y. Zhang, L. Nie, C. Xie and Z. Yan, Colorimetric Detection of Trace Hg^{2+} with Near-Infrared Absorbing Squaraine Functionalized by Dibenzo-18-crown-6 and its Mechanism, *Spectrochim. Acta A Mol. Biomol. Spectrosc.*, 2013, **104**, 87–91; *(j*) K. M. Shafeekh, M. K. A. Rahim, M. C. Basheer, C. H. Suresh and S. Das, Highly Selective and Sensitive Colourimetric Detection of Hg^{2+} Ions by Unsymmetrical Squaraine Dyes, *Dyes and Pigments*, 2013, **96**, 714–721; *(k*) C. Luo, Q. Zhou, B. Zhang and X. Wang, A New Squaraine and Hg^{2+}-based Chemosensor with Tunable Measuring Range for Thiol-Containing Amino Acids, *New J. Chem.*, 2011, **35**, 45–48; *(l*) C. Chen, H. Dong, Y. Chen, L. Guo, Z. Wang, J. J. Sun and N. Fu, Dual-mode Unsymmetrical Squaraine-based Sensor for Selective Detection of Hg^{2+} in Aqueous Media. *Org. Biomol. Chem.*, 2011, **9**, 8195–8201; *(m*) C. Chen, R. Wang, L. Guo, N. Fu, H. Dong, Y. Yuan, A Squaraine-based Colorimetric and "Turn on" Fluorescent Sensor for Selective Detection of Hg^{2+} in an Aqueous Medium, *Org. Lett.*, 2011, **13**, 1162–1165; *(n*) Y. Xu, M. J. Panzner, X. Li, W. J. Youngs and Y. Pang, Host-guest Assembly of Squaraine Dye in Cucurbit[8]uril: Its Implication in Fluorescent Probe for Mercury Ions, *Chem. Commun.*, 2010, **46**, 4073–4075; *(o*) E. M. Nolan and S. J. Lippard, Tools and Tactics for the Optical Detection of Mercuric Ion, *Chem. Rev.*, 2008, **108**, 3443–3480; *(p*) M. C. Basheer, S. Alex, K. G. Thomas, C. H. Suresh and S. Das, A Squaraine-based Chemosensor for Hg^{2+} and Pb^{2+}, *Tetrahedron*, 2006, **62**, 605–610; *(q*) J. V. Ros-Lis, M. D. Marcos, R. Martínez-Máñez, K. Rurack and J. Soto, A Regenerative Chemodosimeter Based on Metal-Induced Dye Formation for the Highly Selective and Sensitive Optical Determination of Hg^{2+} Ions, *Angew. Chem. Inter. Ed.*, 2005, **44**, 4405–4407; *(r*) J. V. Ros-Lis, R. Martínez-Máñez, K. Rurack, F. Sancenón, J. Soto and M. Spieles, Highly Selective Chromogenic Signaling of Hg^{2+} in Aqueous Media at Nanomolar Levels Employing a Squaraine-Based Reporter, *Inorg. Chem.*, 2004, **43**, 5183–5185.

Table S2. Overall (β_i^H) protonation constants of **sbdpa** and dpa in aqueous solution at 298.2±0.1 K and in 0.10±0.01 M KNO_3

Equilibrium reaction	**sbdpa**	dpa[b]
	log β_i^H	
$L + H^+ \rightleftarrows HL^+$	10.85(2)	7.11
$L + 2\ H^+ \rightleftarrows H_2L^{2+}$	14.80(6)	9.59
$L + 3\ H^+ \rightleftarrows H_3L^{3+}$	18.12(4)	–

[a] This work; L denotes the ligand in general; values in parenthesis are standard deviations in the last significant figures. [b] *T* = 293.2 K, *I* = 0.1 M in KNO_3.[28]

Table S3. Overall ($\beta_{M_mH_hL_l}$) stability constants of the complexes of **sbdpa** and dpa with Hg^{2+}, Cu^{2+} and Zn^{2+} in aqueous solution at 298.2 K±0.1 in 0.10±0.01 M KNO_3

Equilibrium reaction[a]	log $\beta_{M_mH_hL_l}$					
	sbdpa			dpa[b]		
	Hg^{2+}	Cu^{2+}	Zn^{2+}	Hg^{2+}	Cu^{2+}	Zn^{2+}
$M^{2+} + H^+ + L \rightleftarrows [M^{II}HL]$	18.06(5)	16.01(3)				
$M^{2+} + L \rightleftarrows [M^{II}L]$	14.60(4)	11.75(4)	8.4(1)		13.85	7.63
$M^{2+} + L \rightleftarrows [M^{II}LOH] + H^+$		3.18(5)				
$M^{II} + L \rightleftarrows [M^{II}L(OH)_2] + 2H^+$		−7.28(6)				
$M^{2+} + 2\ L \rightleftarrows [M^{II}L_2]$				22.25	18.5	12.15
$2\ M^{2+} + H^+ + L \rightleftarrows [M_2^{II}HL]$		19.76(7)	17.84(4)			
$2\ M^{II} + L \rightleftarrows [M_2^{II}L]$	18.97(9)	16.30(7)	13.14(7)			
$2\ M^{II} + L \rightleftarrows [M_2^{II}LOH] + H^+$		9.43(9)	5.9(1)			
$2\ M^{II} + L \rightleftarrows [M_2^{II}L(OH)_2] + 2H^+$		1.64(9)	−1.4(1)			
$2M^{II} + L \rightleftarrows [M_2^{II}L(OH)_3] + 3H^+$		−7.2(1)	−9.5(1)			
$2M^{II} + L \rightleftarrows [M_2^{II}L(OH)_4] + 4H^+$		−17.0(1)	−19.6(1)			

[a] This work; L denotes the ligand in general; values in parenthesis are standard deviations in the last significant figures. [b] *T* = 293.2 K, *I* = 0.1 M in KNO_3, G. Anderegg, E. Hubmann, N. G. Podder and F. Wenk, XI. Pyridinderivate als Komplexbildner. XI. Die Thermodynamik der Metallkomplexbildung mit Bis-, Tris- und Tetrakis [(2-pyridyl)methyl]-aminen, *Helv. Chim. Acta*, 1977, **60**, 123–140.

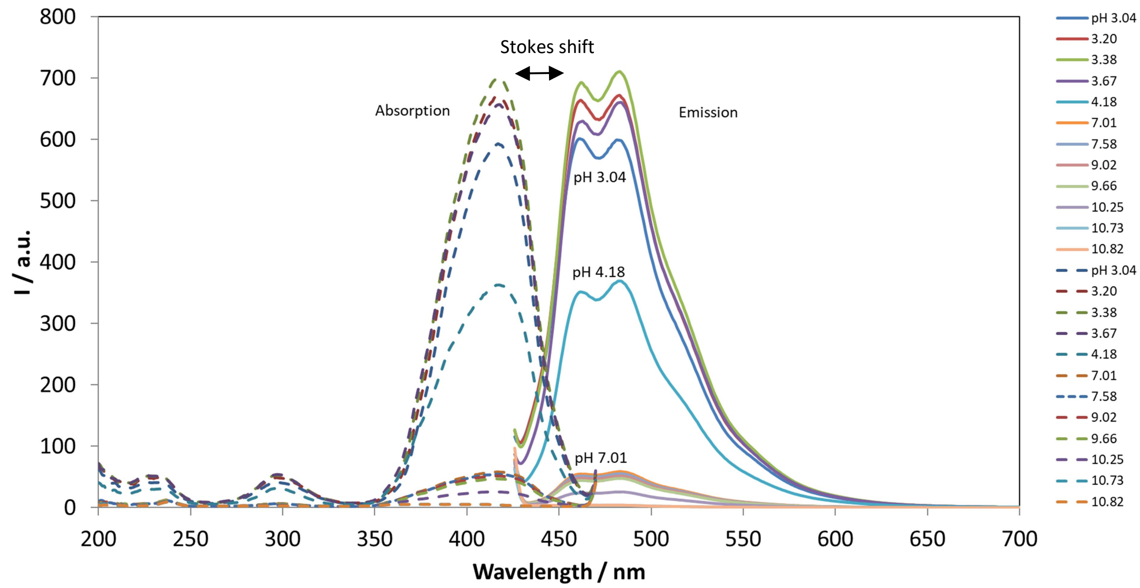

Fig. S1 Absorption and emission spectra of **sbdpa** in aqueous solution with pH variations at $C_L = 1.3\times10^{-3}$ M and $T = 298.2$ K. $\lambda_{exc} = 420$ nm.

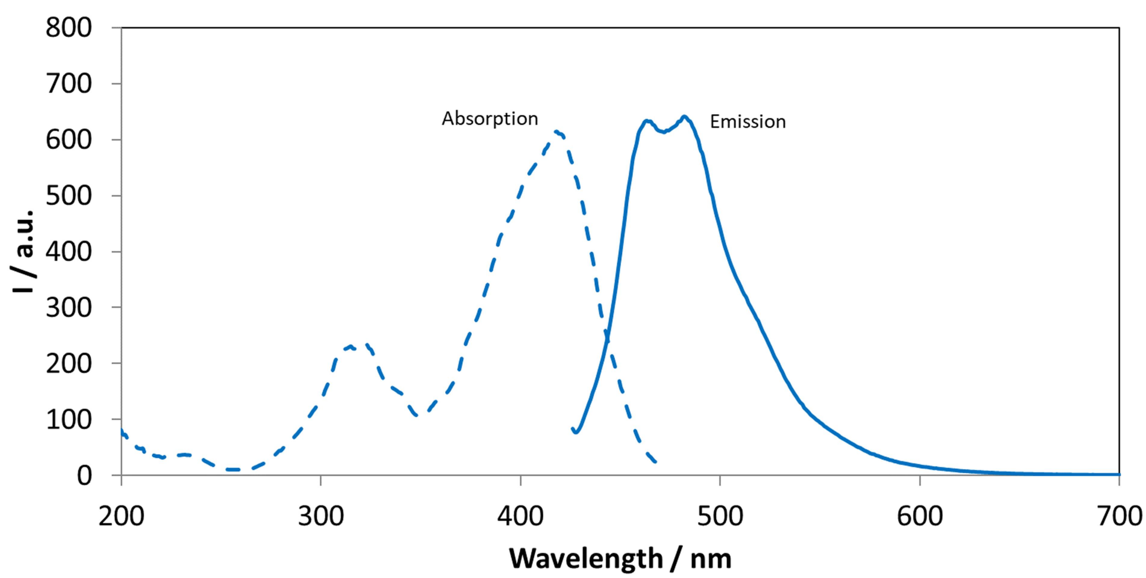

Fig. S2 Absorption and emission spectra of the complex of **sbdpa** with Hg^{2+} 1:1 M:L in aqueous solution at pH 3.1; $C_L = 1.3\times10^{-3}$ M; $T = 298.2$ K. $\lambda_{exc} = 340$ nm.

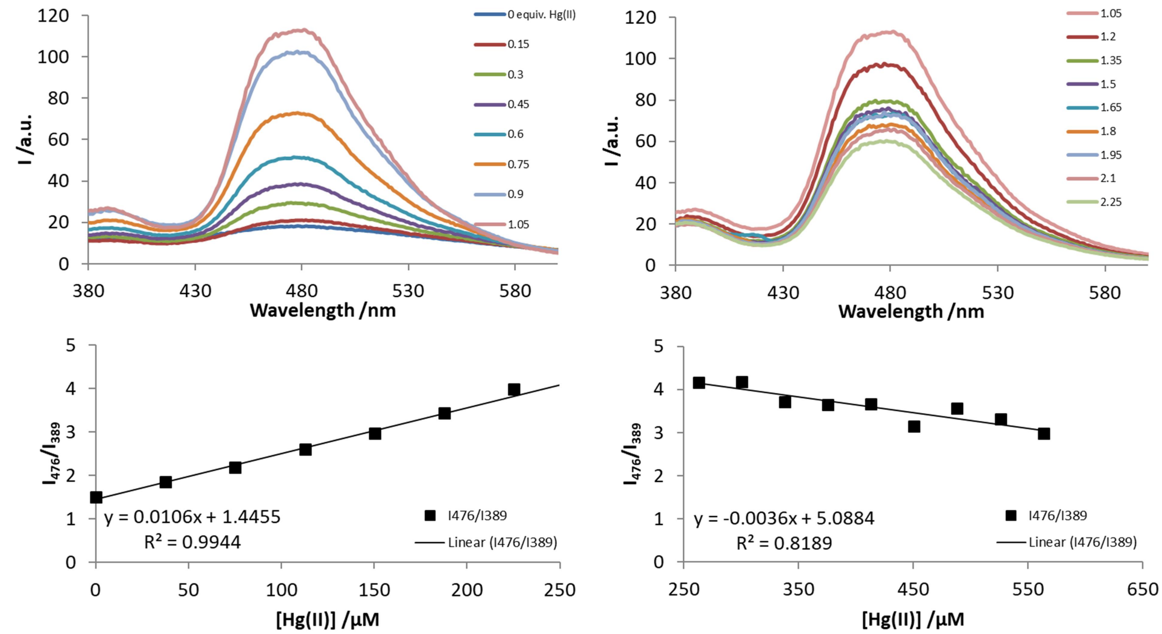

Fig. S3 Fluorescence intensity change of **sbdpa** (2.5×10^{-5} M) upon titration with $Hg(NO_3)_2$ in aqueous buffered solution with MES (2.5×10^{-3} M) at pH 5.0 and T = 298.2 K. λ_{exc} = 340 nm.

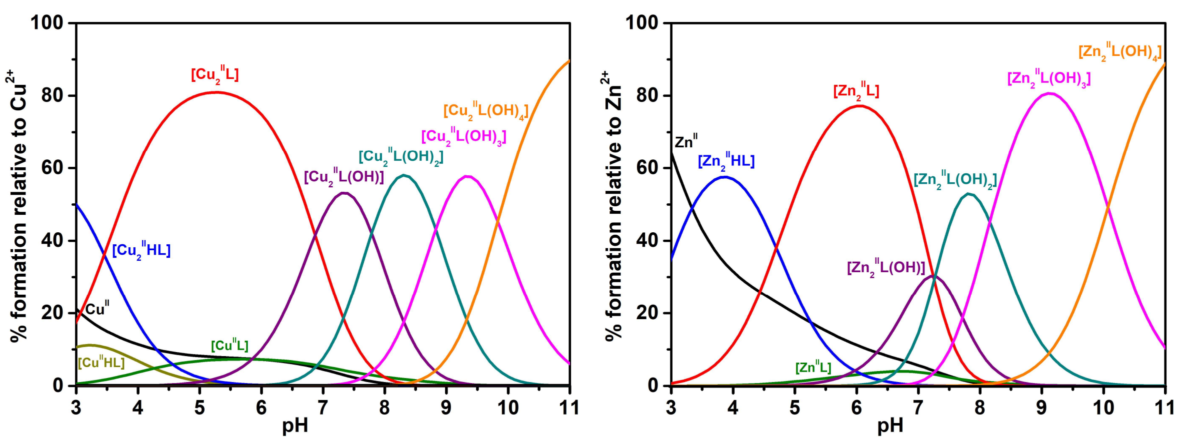

Fig. S4 Species distribution diagrams calculated for the complexes of **sbdpa** with Cu^{2+} and Zn^{2+} cations at 2:1 M:L ratio. $C_M = 2C_L = 2.0\times10^{-3}$ M. L denotes the ligand.

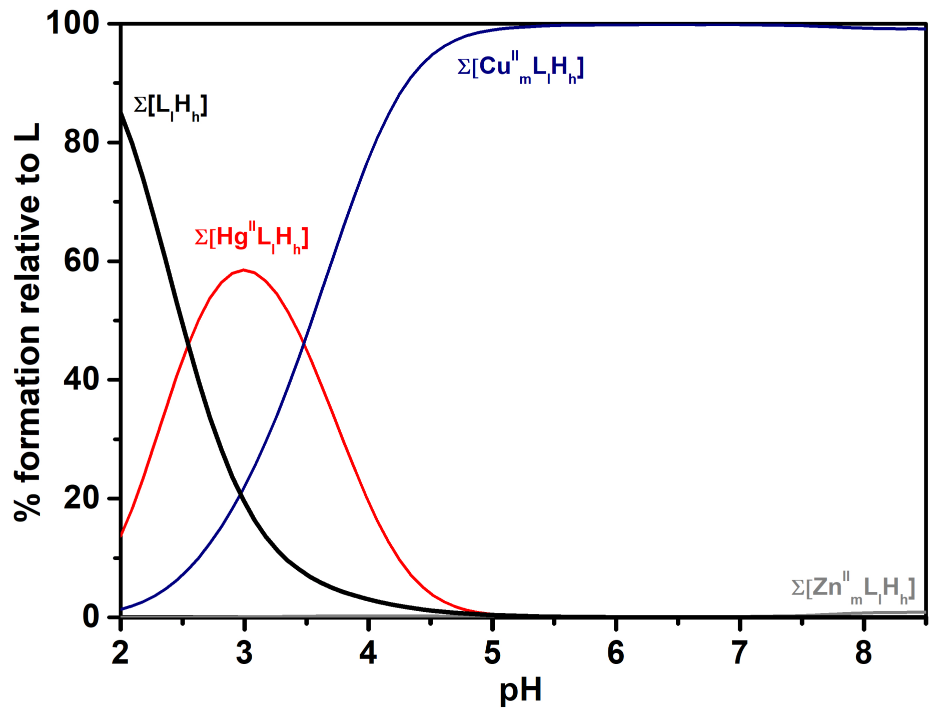

Fig. S5 Competition distribution diagram of the overall amounts of the **sbdpa** in function of pH in presence of Hg^{2+}, Cu^{2+}, and Zn^{2+} in the 1:1:5:5 ratio. $C_{Hg^{2+}} = C_L = 2.5 \times 10^{-5}$ M, $C_{Cu^{2+}} = C_{Zn^{2+}}$ 1.25×10^{-4} M. L denotes the **sbdpa** ligand.

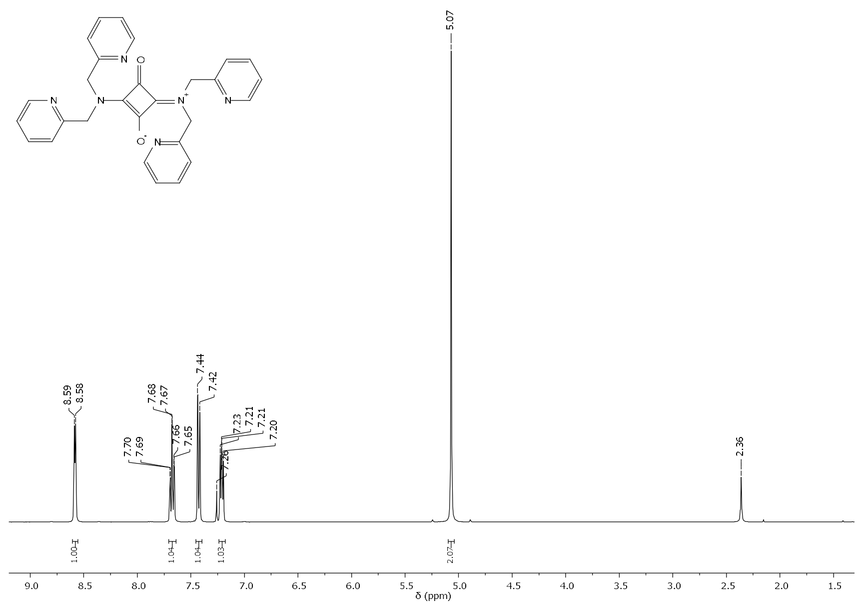

Fig. S6 ^{1}H-NMR spectrum of **sbdpa** in $CDCl_3$.

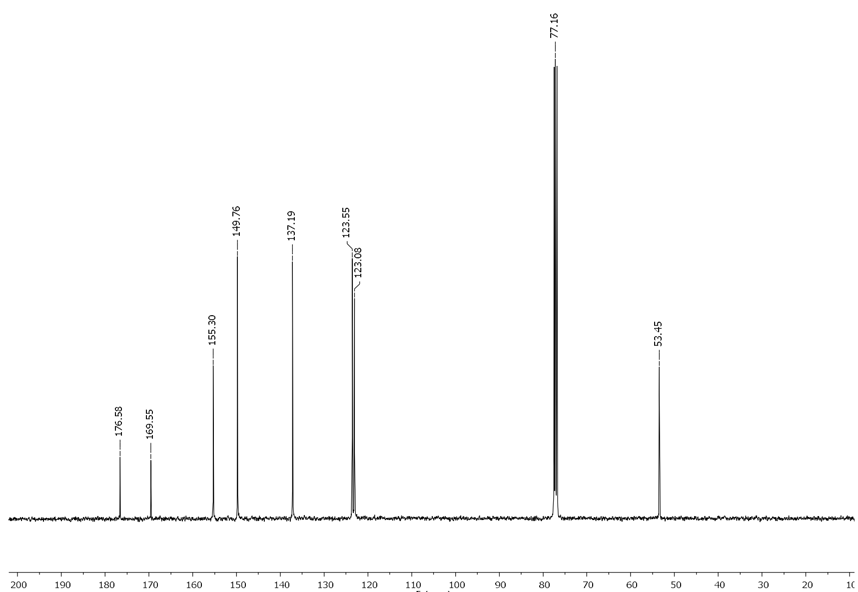

Fig. S7 ^{13}C-NMR spectrum of **sbdpa** in $CDCl_3$.

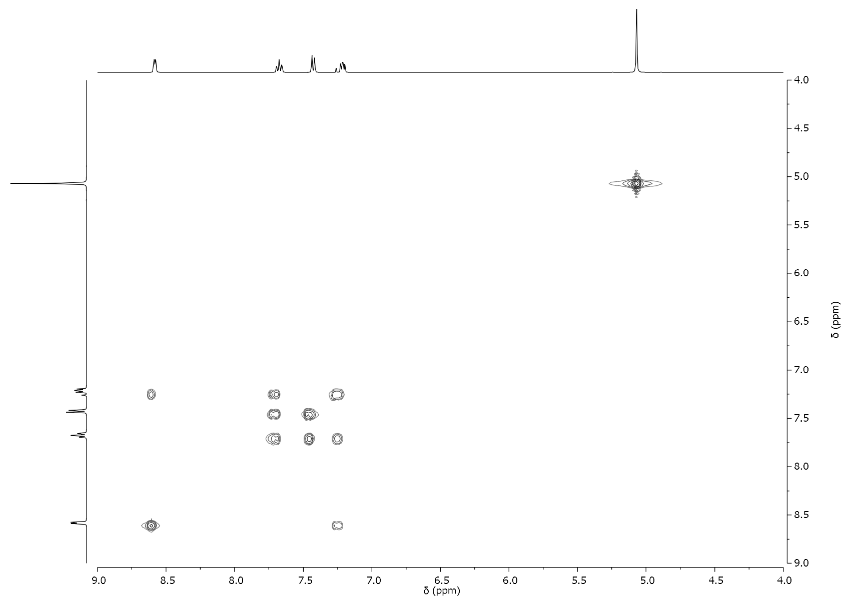

Fig. S8 COSY spectrum of **sbdpa** in $CDCl_3$.

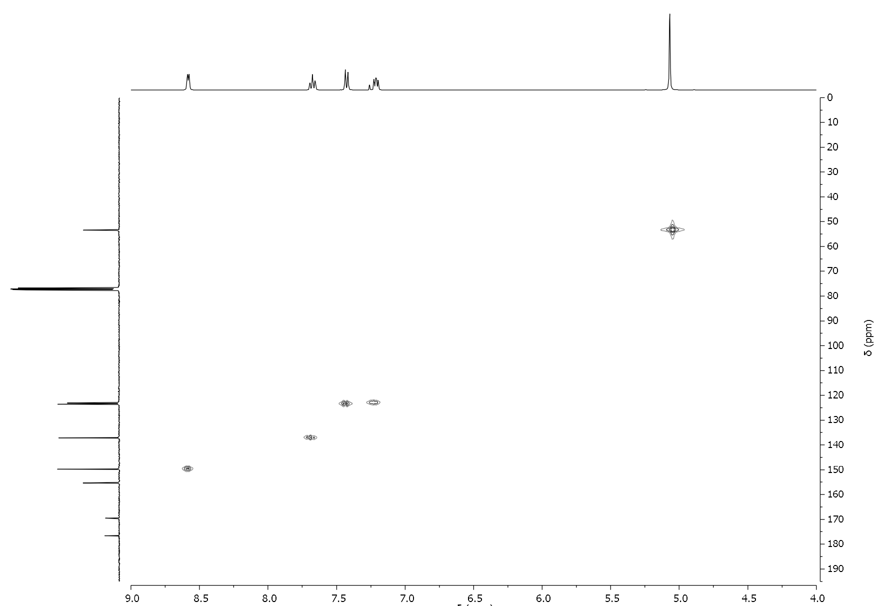

Fig. S9 HMQC spectrum of **sbdpa** in $CDCl_3$.

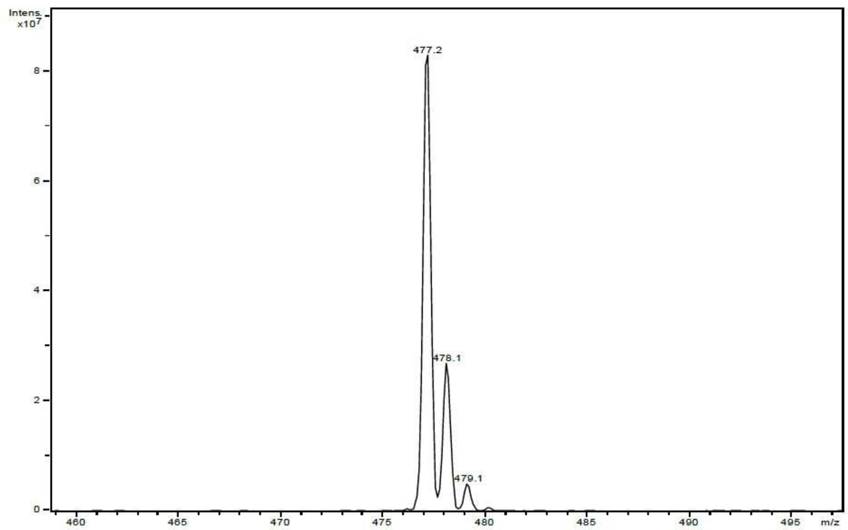

Fig. S10 ESI mass spectrum of **sbdpa** in H_2O/MeOH.

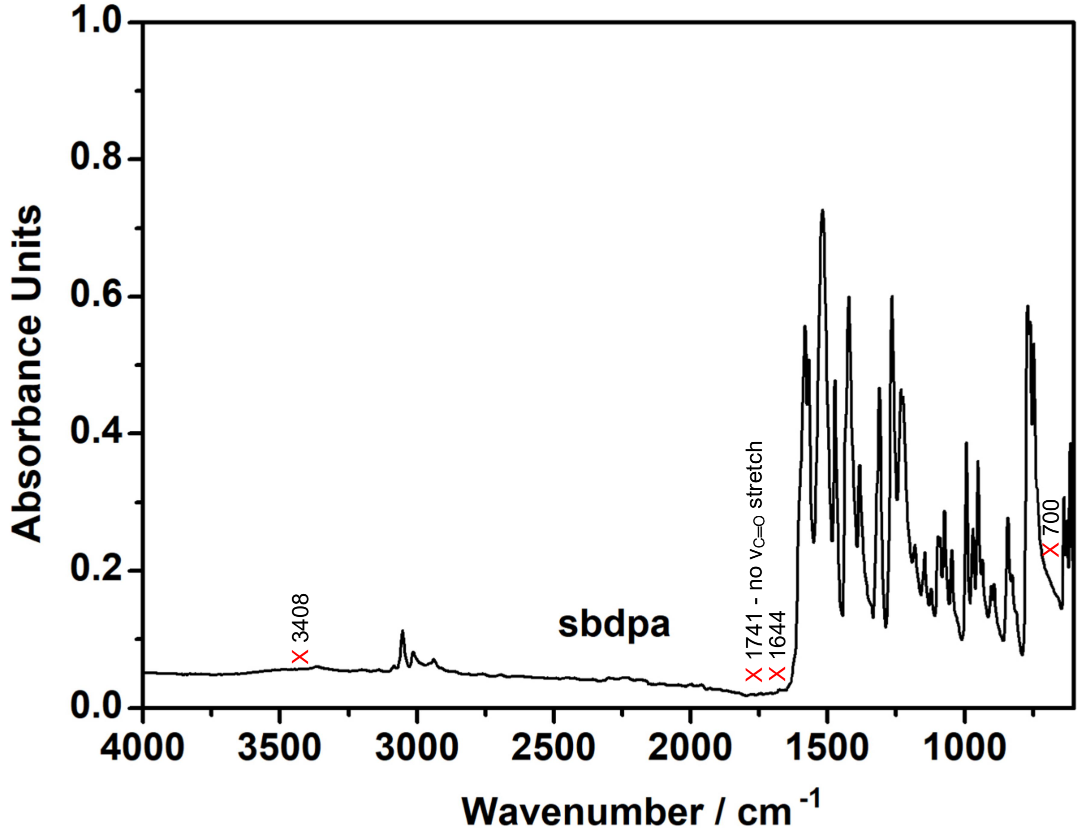

Fig. S11 ATR-FTIR spectrum from **sbdpa** recorded at room temperature; no characteristic $v_{C=O}$ bands found at ≅1700 cm^{-1}, nor typical water bands at 3408, 1644, and 700 cm^{-1}, supporting the fact that sbdpa is in its zwitterionic form, and that it is not an hydrate although it is recrystallized from water.

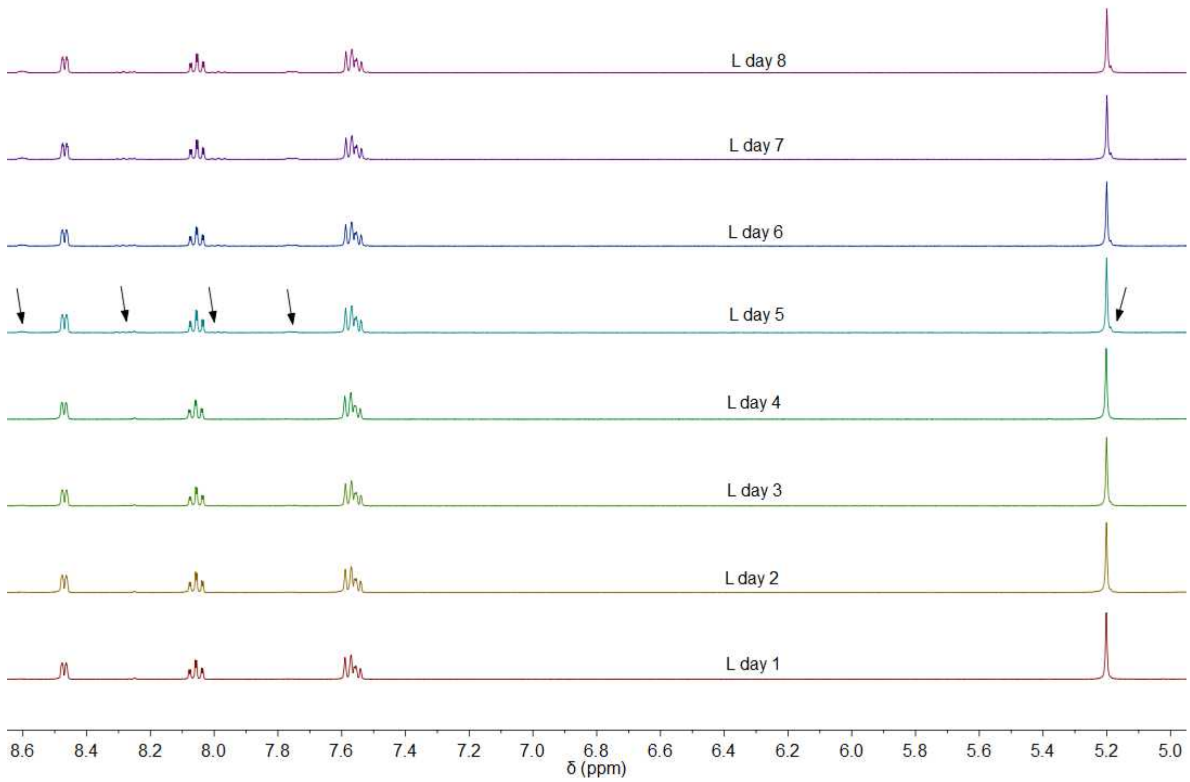

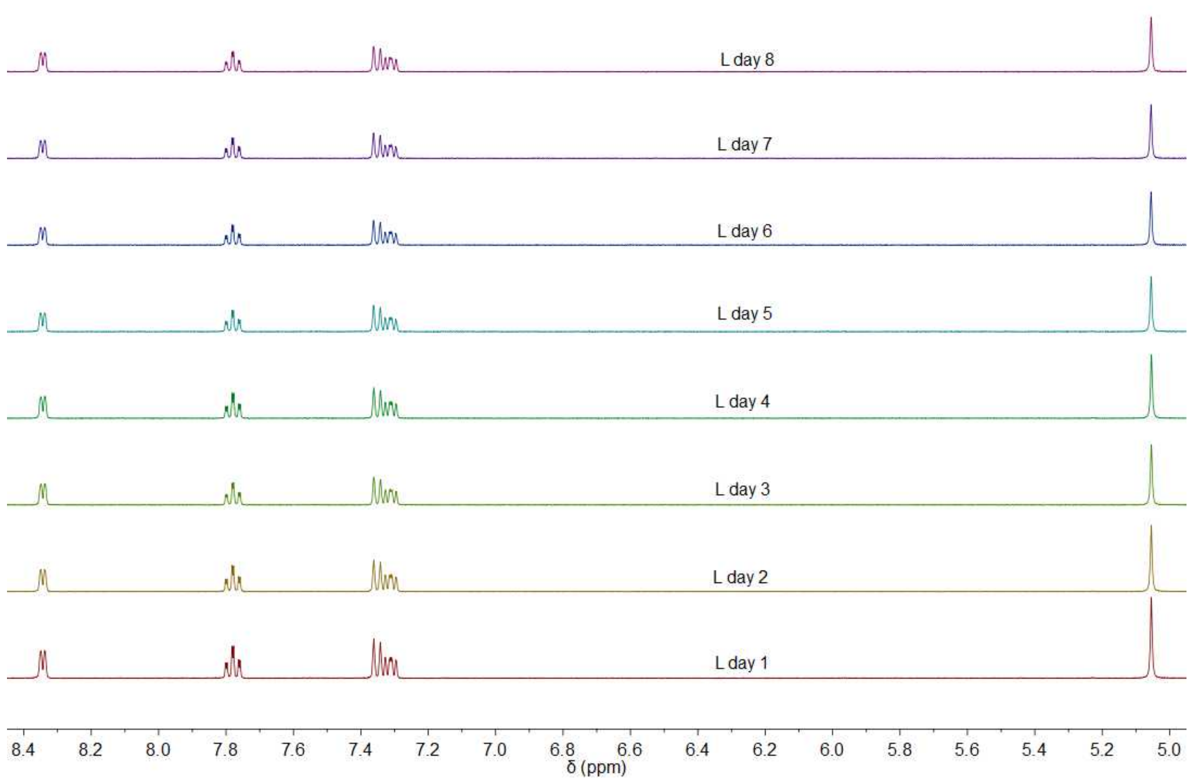

Fig. S12 Evolution of ^{1}H-NMR spectra of **sbdpa** in D_2O with time at pD 3.39 (top) and pD 7.63 (bottom).